LA-UR-23-23576

Khuri-Treiman analysis of $J/\psi \to \pi^+\pi^-\pi^0$

JPAC Collaboration

M. Albaladejo[a] **S. Gonzàlez-Solís**[b] **C. Fernández-Ramírez**[c,d] **N. Hammoud**[e] **V. Mathieu**[f,g] **G. Montaña**[h] **R. J. Perry**[f] **A. Pilloni**[i,j] **A. Rodas**[h] **W. A. Smith**[k,l] **A. Szczepaniak**[h,k,l]

[a] *Instituto de Física Corpuscular (IFIC), Centro Mixto CSIC-Universidad de Valencia, E-46071 Valencia, Spain*

[b] *Theoretical Division, Los Alamos National Laboratory, Los Alamos, NM 87545, USA*

[c] *Departamento de Física Interdisciplinar, Universidad Nacional de Educación a Distancia (UNED), Madrid E-28040, Spain*

[d] *Instituto de Ciencias Nucleares, Universidad Nacional Autónoma de México, Ciudad de México 04510, Mexico*

[e] *Institute of Nuclear Physics, Polish Academy of Sciences, 31-342 Kraków, Poland*

[f] *Departament de Física Quàntica i Astrofísica and Institut de Ciències del Cosmos, Universitat de Barcelona, E08028, Spain*

[g] *Departamento de Física Teórica, Universidad Complutense de Madrid and IPARCOS, 28040 Madrid, Spain*

[h] *Theory Center, Thomas Jefferson National Accelerator Facility, Newport News, VA 23606, USA*

[i] *Dipartimento di Scienze Matematiche e Informatiche, Scienze Fisiche e Scienze della Terra, Università degli Studi di Messina, I-98122 Messina, Italy*

[j] *INFN Sezione di Catania, I-95123 Catania, Italy*

[k] *Department of Physics, Indiana University, Bloomington, IN 47405, USA*

[l] *Center for Exploration of Energy and Matter, Indiana University, Bloomington, IN 47403, USA*

E-mail: sergig@lanl.gov

Abstract: We study the decay $J/\psi \to \pi^+\pi^-\pi^0$ within the framework of the Khuri-Treiman equations. We find that the BESIII experimental di-pion mass distribution in the $\rho(770)$-region is well reproduced with a once-subtracted P-wave amplitude. Furthermore, we show that F-wave contributions to the amplitude improve the description of the data in the $\pi\pi$ mass region around 1.5 GeV. We also present predictions for the $J/\psi \to \pi^0\gamma^*$ transition form factor.

Contents

1 Introduction

Decays of the lowest-lying charmonium states provide an excellent environment to study light hadron spectroscopy, search for exotic mesons, test QCD and QCD-based models, as well as testing theoretical techniques in a region where both non-perturbative and perturbative QCD effects play a role.

In this work we analyze the decay $J/\psi \to \pi^+\pi^-\pi^0$, to study the dynamics of the three-pion system at low and intermediate energies under rather clean conditions. Here, the final state invariant mass distribution can contain contributions from the P-wave ($J^{PC} = 1^{--}$) and F-wave ($J^{PC} = 3^{--}$) states of the $\pi\pi$ subsystem. Previous experimental studies from BESII [1] and BABAR [2] showed that the P-wave $\rho(770)\pi$ intermediate state dominates the process, but limited statistics prevented any detailed study of substructures in the 3π system. While the dominance of the $\rho(770)$ resonance can be clearly seen in the Dalitz plot distribution and projection measurements by the BESIII collaboration obtained with roughly 1.9 million $J/\psi \to \pi^+\pi^-\pi^0$ events [3], there are hints of contributions other than the $\rho(770)$. For example, the absence of events in the center of the Dalitz plot indicates the contribution from additional states and/or partial waves which may interfere destructively with the $\rho(770)$. Exactly the opposite situation is found for the partner reaction $\psi(2S) \to \pi^+\pi^-\pi^0$. There, the 7872 events from BESIII [3] show a completely different shape of the $\pi\pi$ invariant mass distribution and the Dalitz plot — the $\rho\pi$ contribution is subleading and almost all events are found in the center of the Dalitz plot, with data indicating that the main contribution comes from a higher mass resonance, *i.e.* the $\rho(2150)$ resonance with $J^{PC} = 1^{--}$. The different picture between the J/ψ and $\psi(2S)$ decays into $\pi^+\pi^-\pi^0$ is known as the $\rho\pi$ puzzle and still remains largely unresolved (see *e.g.* [4–8], and references therein). New high-statistics BESIII data on J/ψ decays will soon be available [9, 10], which could be used to greatly improve the theoretical uncertainties associated to vector charmonium decays. In particular, they might help clarify the $\rho\pi$ puzzle, as well as provide access to high-precision ρ-ω mixing effect analyses and motivate coupled channel studies with the decays $J/\psi \to K^+K^-\pi^0$ and $J/\psi \to K_S K^\pm\pi^\mp$.

The decay $J/\psi \to \pi^+\pi^-\pi^0$ has previously been studied within the context of the Veneziano model [11], and using aspects of unitarity and analyticity constraints [12, 13]. Here, we adapt the Khuri-Treiman (KT) framework [14], applied extensively in the isospin-violating decay $\eta \to 3\pi$ [15–21] and in the decay of light vector isoscalar resonances $\omega, \phi \to 3\pi$ [22–24], to the analysis of the vector charmonium decay $J/\psi \to \pi^+\pi^-\pi^0$. We show that one subtraction in the KT equations satisfactorily describes the BESIII experimental di-pion mass distribution at the peak of the $\rho(770)$. In addition, we find that F-wave effects are needed to describe the intermediate energy region around 1.5 GeV. We also apply our analysis techniques to predict the $J/\psi \to \pi^0\gamma^*$ transition form factor. Our study lays the groundwork for a detailed analysis of J/ψ decays using the large data sample currently being collected at BESIII.

This paper is organized as follows. In Section 2 we review the KT formalism for the $J/\psi \to 3\pi$ decay. In Section 3 we apply the formalism to the BESIII data and discuss the results. In Section 4, we present predictions for the $J/\psi \to \pi^0\gamma^*$ transition form factor,

and we summarize our findings in Section 5.

2 Formalism

2.1 Decay amplitude and kinematics

The amplitude for the decay $J/\psi(p_V) \to \pi^0(p_0)\,\pi^+(p_+)\,\pi^-(p_-)$ can be expressed in terms of a kinematic prefactor and a single invariant scalar function $F(s,t,u)$ containing the dynamical information,

$$\mathcal{M}(s,t,u) = i\,\epsilon_{\mu\nu\alpha\beta}\,\epsilon^{\mu}(p_V)\,p_+^{\nu}\,p_-^{\alpha}\,p_0^{\beta}\;F(s,t,u)\,, \tag{2.1}$$

where $\epsilon_{\mu\nu\alpha\beta}$ is the Levi-Civita tensor and $\epsilon^{\mu}(p_V)$ is the polarization vector of the J/ψ meson. The particle momenta are related to the Mandelstam variables through:

$$s = (p_+ + p_-)^2\,, \quad t = (p_0 + p_+)^2\,, \quad u = (p_0 + p_-)^2\,, \tag{2.2}$$

with $s + t + u = m_{J/\psi}^2 + 3m_\pi^2$. In this manuscript, we work in the isospin limit with $m_\pi \doteq m_{\pi^\pm} = m_{\pi^0}$ and $m_\pi = (2m_{\pi^\pm} + m_{\pi^0})/3$. **Arkaitz: A bit of a pedantic request, what is the pion mass used? Sergi: added to be specific.** The scattering angle in the s-channel, defined by the center of mass of the $\pi^+\pi^-$ pair, is denoted by θ_s and is given by:

$$\cos\theta_s(s,t,u) = \frac{t-u}{4\,p(s)\,q(s)}\,, \quad \sin\theta_s(s,t,u) = \frac{\sqrt{\phi(s,t,u)}}{2\sqrt{s}\,p(s)\,q(s)}\,, \tag{2.3}$$

where the momenta $p(s)$ and $q(s)$,

$$p(s) = \frac{\lambda^{\frac{1}{2}}(s,m_\pi^2,m_\pi^2)}{2\sqrt{s}}\,, \quad q(s) = \frac{\lambda^{\frac{1}{2}}(s,m_{J/\psi}^2,m_\pi^2)}{2\sqrt{s}}\,, \tag{2.4}$$

are, respectively, the momenta of the $\pi^\pm$ and π^0 in the s-channel. $\lambda(a,b,c) = a^2 + b^2 + c^2 - 2ab - 2bc - 2ca$ is the Källén, or triangle, function [25]. The zeroes of the well-known Kibble function [26] ,

$$\phi(s,t,u) = (2\sqrt{s}\;\sin\theta_s\;p(s)\,q(s))^2 = s\,t\,u - m_\pi^2(m_{J/\psi}^2 - m_\pi^2)^2\;, \tag{2.5}$$

define the boundaries of the physical regions of the process. The Dalitz-plot boundaries in t for a given value of s for $J/\psi \to 3\pi$ lie within the interval $[t_{\rm min}(s),\; t_{\rm max}(s)]$, with

$$t_{\rm max,min}(s) = \frac{m_{J/\psi}^2 + 3m_\pi^2 - s}{2} \pm 2\,p(s)\,q(s)\;, \tag{2.6}$$

while the allowed range for s is given by $s_{\rm min} = 4m_\pi^2$ to $s_{\rm max} = (m_{J/\psi} - m_\pi)^2$.

Finally, the measured differential decay width can be written in terms of the invariant amplitude $F(s,t,u)$ as

$$\frac{d^2\Gamma}{ds\,dt} = \frac{1}{(2\pi)^3}\,\frac{1}{32\,m_{J/\psi}^3}\,\frac{1}{3}\,\frac{\phi(s,t,u)}{4}\;|F(s,t,u)|^2\,. \tag{2.7}$$

2.2 Khuri–Treiman equations for $J/\psi \to 3\pi$

The KT formalism for the $J/\psi \to 3\pi$ amplitude $F(s,t,u)$ is formally identical to the well-established one for the $\omega \to 3\pi$ decay amplitude [22–24, 27], and has been discussed in [28] (see also Ref. [29]). As shown in these references, the s-channel partial-wave expansion for $F(s,t,u)$ is given by

$$F(s,t,u) = \sum_{J\,\text{odd}}^{\infty} (p(s)\,q(s))^{J-1}\; P'_J(z_s)\; f_J(s)\,, \tag{2.8}$$

where $z_s = \cos\theta_s$ and $P'_J(z_s)$ is the differentiated Legendre polynomial. The KT representation of the scalar function $F(s,t,u)$ in Eq. (2.8) may be obtained by replacing the infinite sum of partial waves in the s-channel with the sum of three so-called isobar amplitudes, one for each of the s-, t- and u-channels. By truncating the partial wave expansion of each isobar amplitude at $J_{\max} = 1$ we obtain the following crossing-symmetric isobar decomposition [22, 23, 30]:

$$F(s,t,u) = F_1(s) + F_1(t) + F_1(u)\,, \tag{2.9}$$

where each isobar amplitude, $F_1(x)$, has only a right-hand or unitary cut in its respective Mandelstam variable. The relation between $F_1(s)$ and $f_1(s)$ is obtained by projecting Eq. (2.9) onto the s-channel partial wave,

$$f_1(s) = F_1(s) + \hat{F}_1(s)\,, \tag{2.10}$$

$$\hat{F}_1(s) \equiv 3\int_{-1}^{1} \frac{dz_s}{2}\,(1-z_s^2)\,F_1(t(s,z_s))\,, \tag{2.11}$$

where the inhomogeneity, $\hat{F}_1(s)$, contains the s-channel projection of the left-hand cut contributions due to the t- and u-channels, and its evaluation in the decay region requires a proper analytical continuation [31]. Assuming elastic unitarity with only two-pion intermediate states, we arrive at the KT equation for the $J/\psi \to 3\pi$ decay, *i.e.* the unitarity relation for the isobar amplitude $F_1(s)$:

$$\text{disc}\,F_1(s) = 2i\left(F_1(s) + \hat{F}_1(s)\right)\,\sin\delta_1(s)\,e^{-i\delta_1(s)}\,\theta(s-4m_\pi^2)\,, \tag{2.12}$$

where $\delta_1(s)$ is the P-wave $\pi\pi$ phase shift, which is real.

Given the discontinuity relation in Eq. (2.12), one can write an unsubtracted dispersion relation for $F_1(s)$ as

$$F_1(s) = \frac{1}{2\pi i}\int_{4m_\pi^2}^{\infty} ds'\,\frac{\text{disc}\,F_1(s')}{s'-s}\,, \tag{2.13}$$

the solution of which can be written as:

$$F_1(s) = \Omega_1(s)\left(a + \frac{s}{\pi}\int_{4m_\pi^2}^{\infty}\frac{ds'}{s'}\frac{\sin\delta_1(s')\,\hat{F}_1(s')}{|\Omega_1(s')|\,(s'-s)}\right)\,, \tag{2.14}$$

where $\Omega_1(s)$ is the usual Omnès function [32],

$$\Omega_1(s) = \exp\left[\frac{s}{\pi}\int_{4m_\pi^2}^{\infty}\frac{ds'}{s'}\frac{\delta_1(s')}{s'-s}\right]. \tag{2.15}$$

The subtraction constant a in Eq. (2.14) is the only free parameter in the model. It is in general complex, $a = |a|\,e^{i\phi_a}$. While its modulus $|a|$ can be fixed from the experimental $J/\psi \to 3\pi$ decay width using data, no observable of the decay is sensitive to the overall phase ϕ_a, so we can set $\phi_a = 0$. Since it determines the overall normalization of the amplitude, the constant a can be factored out.

We note that due to the asymptotic behavior of $F_1(s)$ in Eq. (2.14), the amplitude $F(s,t,u)$ satisfies the Froissart-Martin bound [22, 33, 34]. Also note that, even though $F_1(s)/\Omega_1(s)$ in Eq. (2.14) looks like a once-subtracted dispersion relation, $F_1(s)$ actually satisfies the unsubtracted dispersion relation given in Eq. (2.13). Therefore, the energy dependence of $F_1(s)$ is a pure prediction given solely by the phase shift $\delta_1(s)$. Here, we take $\delta_1(s)$ from the phase shift parametrizations of Ref. [35] that are valid roughly up to $\sqrt{s} = 2$ GeV. Therefore, the phase shift that we employ contains the physics of the $\rho(770)$ and also the effects of the higher $\rho(1450)$ and $\rho(1770)$ resonances. For our analysis, beyond $\Lambda \equiv \sqrt{s} = 1.85$ GeV we smoothly guide the $\delta_1(s)$ to π through [27, 36]

$$\delta_\infty(s) \equiv \lim_{s\to\infty}\delta_1(s) = \pi - \frac{\alpha}{\beta + (s/\Lambda^2)^{3/2}}, \tag{2.16}$$

where α and β are parameters introduced so that the phase $\delta_1(s)$ and its first derivative $\delta'(s)$ are continuous at $s = \Lambda^2$. Their explicit expressions read

$$\alpha = \frac{3\left(\pi - \delta_1(\Lambda^2)\right)^2}{2\Lambda^2\delta_1'(\Lambda^2)}, \quad \beta = -1 + \frac{3\left(\pi - \delta_1(\Lambda^2)\right)}{2\Lambda^2\delta_1'(\Lambda^2)}. \tag{2.17}$$

This ensures the expected asymptotic $1/s$ behavior of $\Omega_1(s)$. The phase shifts $\delta_1(s)$ that we use as an input are shown in Fig. 1 up to 2.5 GeV. There are several solutions for the phase shifts in Ref. [35]. We use solution I (solid black line) as our central input for the phase and use solutions II (dashed blue line) and III (dot-dashed green line) to quantify the systematic uncertainties in our calculations. The solution of Ref. [37] (dotted red line) is valid up to about 1.3 GeV, and is also shown in the figure for completeness.

We solve Eq. (2.14) following a numerical iterative procedure similar to Refs. [16, 20–22, 38]. We use $F_1(s) = \Omega_1(s)$ as an efficient initial input to calculate $\hat{F}_1(s)$ from Eq. (2.11), which subsequently is inserted as an input in Eq. (2.14) for the computation of an updated $F_1(s)$. This cyclic calculation is repeated until the solution converges. In Fig. 2, we show the solutions for $F_1(s)$ (normalized to $a = 1$) after each iteration step along with the initial input (dashed blue line). As can be seen, convergence is achieved after three iterations. The difference between the final solution (solid black) and the starting point, *i.e.* $F_1(s) = \Omega_1(s)$ (dashed blue), is rather small, hinting at moderate crossed-channel effects.

Note that when the crossed-channel rescattering effects are removed from the isobar $F_1(s)$, *i.e.* when $\hat{F}_1(s) = 0$ in Eq. (2.14), $F_1(s)$ is simply the pure Omnès function multiplied

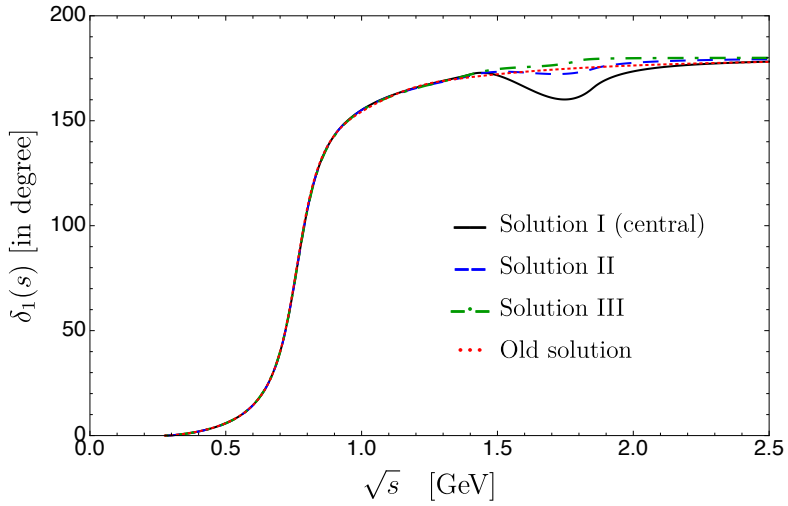

Figure 1. Solutions I, II and III for the P-wave phase shift $\delta_1(s)$ from Ref. [35] valid roughly up to $\sqrt{s} = 2$ GeV. The solution of Ref. [37] (dotted red line) is valid up to about $\sqrt{s} = 1.3$ GeV, and is shown for completeness.

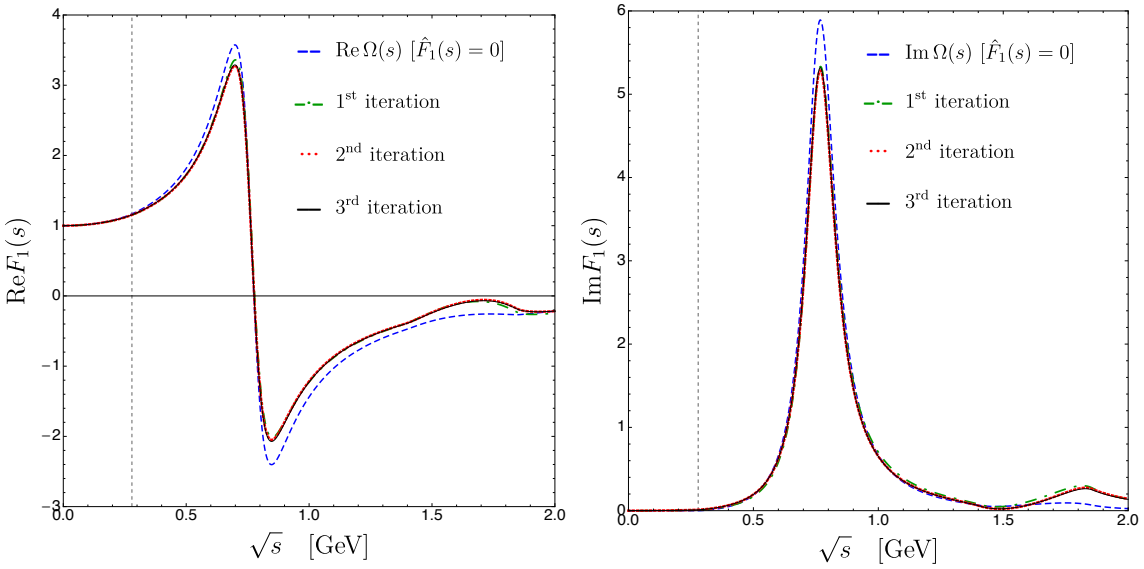

Figure 2. Convergence behavior of the iterative procedure for the real (left plot) and imaginary (right plot) parts of the amplitude $F_1(s)$ given in Eq. (2.14). The vertical line denotes the two-pion threshold.

by a constant,

$$F_1(s) = a' \Omega_1(s) \,, \tag{2.18}$$

which implies the following isobar decomposition of the full amplitude (*cf.* Eq. (2.9)):

$$F(s,t,u) = a' \left(\Omega_1(s) + \Omega_1(t) + \Omega_1(u) \right) \,. \tag{2.19}$$

In this case, a new normalization constant a' has to be chosen to reproduce the $J/\psi \to 3\pi$ decay width. Also note that Eq. (2.14) can be written in the form

$$F_1(s) = \Omega_1(s) \left(a + b' \, s + \frac{s^2}{\pi} \int_{4m_\pi^2}^{\infty} \frac{ds'}{(s')^2} \frac{\sin\delta_1(s') \, \hat{F}_1(s')}{|\Omega_1(s')| \, (s'-s)} \right) \,, \tag{2.20}$$

where b' satisfies the following sum rule [22]:

$$b \equiv b'/a = \frac{1}{\pi} \int_{4m_\pi^2}^{\infty} \frac{ds'}{(s')^2} \frac{\sin\delta_1(s') \, \hat{F}_1(s')/a}{|\Omega_1(s')|} \,. \tag{2.21}$$

The subtraction constant, b, is complex due to the presence of the three-particle cut in the physical region of the decay amplitude. This value is found to be:

$$b_{\rm sum} \simeq 0.141 \, e^{2.321\, i} \ {\rm GeV}^{-2} \,. \tag{2.22}$$

Had we used solution II or III of the phase shift $\delta_1(s)$ (*cf.* Fig. 1), we would have obtained $b_{\rm sum} \simeq 0.129 \, e^{2.640\, i}$ GeV^{-2} and $b_{\rm sum} \simeq 0.124 \, e^{2.811\, i}$ GeV^{-2}, respectively.

Performing a subtraction on the dispersive solution in Eq. (2.13) leads to the expression [20, 22, 30]:

$$F_1(s) = a \left[F_a(s) + b \, F_b(s) \right] \,, \tag{2.23a}$$

where now b is not constrained to satisfy Eq. (2.21), and the functions $F_a(s)$ and $F_b(s)$ are given by

$$F_a(s) = \Omega_1(s) \left[1 + \frac{s^2}{\pi} \int_{4m_\pi^2}^{\infty} \frac{ds'}{s'^2} \frac{\sin\delta_1(s') \, \hat{F}_a(s')}{|\Omega_1(s')|(s'-s)} \right] \,, \tag{2.23b}$$

$$F_b(s) = \Omega_1(s) \left[s + \frac{s^2}{\pi} \int_{4m_\pi^2}^{\infty} \frac{ds'}{s'^2} \frac{\sin\delta_1(s') \, \hat{F}_b(s')}{|\Omega_1(s')|(s'-s)} \right] \,. \tag{2.23c}$$

These functions only need to be calculated once since they are independent of the numerical values of a and b and, as we will discuss in Sec. 3, a and b will become fit parameters. In Fig. 3, we show the solutions for $F_a(s)$ and $F_b(s)$ using a numerical iterative procedure similar to the one described previously. In this case, nine iterations are needed to obtain convergent solutions. Strictly speaking, the amplitude $F(s,t,u)$ built from $F_1(s)$ in Eq. (2.23a) does not satisfy the asymptotic Froissart-Martin bound for an arbitrary value of the parameter $b \neq b_{\rm sum}$ [*cf.* Eq. (2.22)]. The main advantage of introducing one subtraction is that, due to the additional $1/s'$ factor introduced, we reduce the importance of the high energy region of the dispersion integrals where the phase shift is not well-known. By letting the subtraction constant b be a free parameter, we can partially absorb our ignorance of the higher energy part of the integral. This allows us to parametrize some unknown energy dependence of the $J/\psi \to 3\pi$ interaction not directly related to $\pi\pi$ rescattering. As we will show in the following section, the once-subtracted parametrization provides an excellent representation of the data from BESIII in the $\rho(770)$ resonance region.

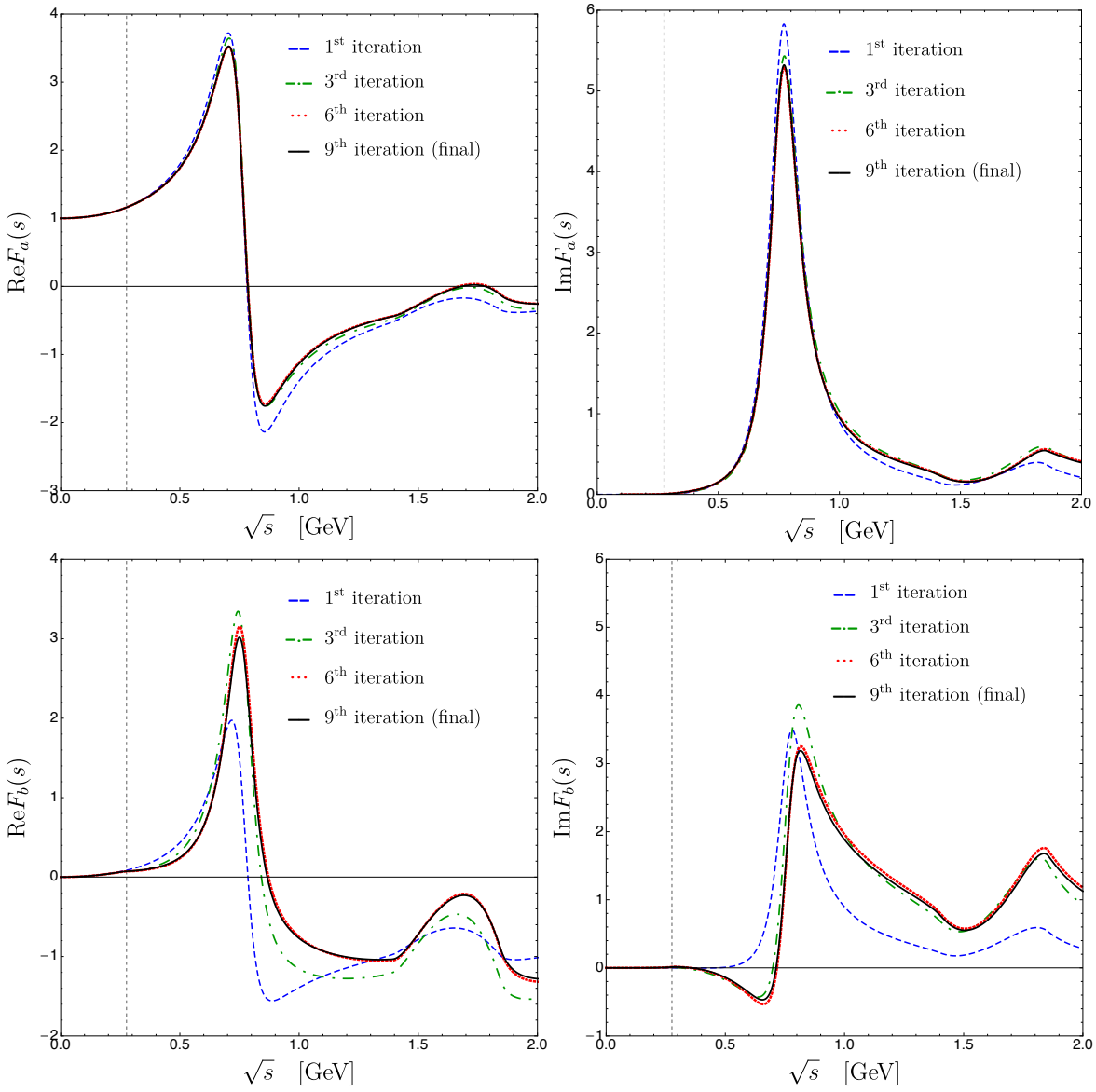

Figure 3. Convergence behavior of the iterative procedure for the real (left plots) and imaginary (right plots) parts of the amplitudes $F_a(s)$ (Eq. (2.23b), upper plots) and $F_b(s)$ (Eq. (2.23c), lower plots). The vertical line denotes the two-pion threshold.

3 Results

3.1 *P*-wave contribution

We now compare our KT amplitudes defined in the previous section to the experimental data from the BESIII collaboration [3]. Given that the Dalitz plot distribution is not publicly available, we are only able to analyze the di-pion mass projection of Eq. (2.7), computed on the $s \equiv m_{\pi\pi}^2 = (p_+ + p_-)^2$ invariant mass. We start by using the unsubtracted KT amplitude Eq. (2.14). The single free parameter a only affects the overall normalization

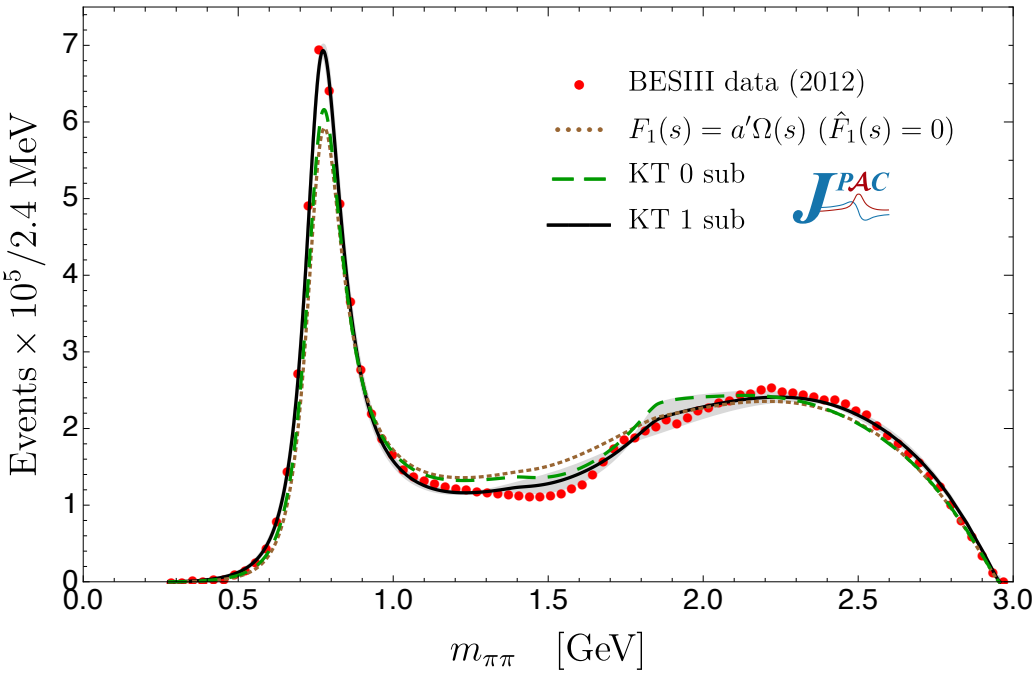

Figure 4. BESIII (red circles) [3] measurement of the $m_{\pi\pi}$ invariant mass distribution for the decay $J/\psi \to 3\pi$ as compared to our prediction without crossed-channel effects (dotted brown line), with the unsubtracted KT amplitude (dashed green line) and our fit in Eq. (3.2) including one subtraction (black solid line).

of the amplitude and can be fixed from the $J/\psi \to \pi^+\pi^-\pi^0$ decay width. Using the PDG values $\Gamma_{J/\psi} = 92.6$ keV and $\text{BR}(J/\psi \to \pi^+\pi^-\pi^0) = 2.10(8)\%$ [39] one finds $|a| \simeq 0.051$ GeV^{-3}. In Fig. 4, we compare our prediction, denoted as KT 0 sub (dashed green line), to the $m_{\pi\pi}$ distribution of the measured number of events by BESIII (red circles) with proper normalization (*cf.* Eq. (3.1)). In the figure, we also show the result obtained when the crossed-channel rescattering is neglected (*cf.* Eq. (2.19)), in which case the global normalization is found to be $|a'| \simeq 0.046$ GeV^{-3}. As can be observed, the result of the Omnès solution (dotted brown line) lies below that of the unsubtracted KT $F_1(s)$ solution at the peak of the ρ-meson, and neither reproduce the experimental data in this region. In addition, both appear to fail at describing the intermediate energy region. In order to achieve a better description of the data, we next use the more flexible, once-subtracted amplitude Eqs. (2.23b) and (2.23c), with the additional subtraction constant b fitted to BESIII data. For our analysis, we define

$$\chi^2_{\text{data}} = \sum_{i=1} \left(\frac{N_{\text{ev},i} - \mathcal{N} d\Gamma_i^{\text{th}}/dm_{\pi\pi}}{\sigma_{N_{\text{ev},i}}} \right)^2 , \tag{3.1}$$

where $N_{\text{ev},i}$ and $\sigma_{N_{\text{ev},i}}$ are, respectively, the experimental number of events distribution and the corresponding error in the i-th bin and $d\Gamma_i^{\text{th}}/dm_{\pi\pi}$ is the theoretical expression for the decay distribution (*cf.* Eq. (2.7)). The constant $\mathcal{N}$ is at this stage an arbitrary normalization. Since we are not determining the branching ratio, we reabsorb the global

normalization of the amplitude a into $\mathcal{N}$ and fix alone this overall constant from the fit to the BESIII data. The sum in Eq. (3.1) runs over the 80 data points.

The $\chi^2_{\rm data}$ minimization yields

$$|b| = 0.198(1)(35)\ \text{GeV}^{-2}\,, \quad \phi_b = 2.675(3)(300)\,, \tag{3.2}$$

which implies $|a| = 0.0565(0)(22)\ \text{GeV}^{-3}$ for the normalization of the amplitude upon using the BR$(J/\psi \to \pi^+\pi^-\pi^0)$ from the PDG. The first error is statistical and the second one is the theoretical systematic uncertainty attached to our calculations. The latter is obtained from the absolute value of the difference between the fits performed with solutions I (central solution) and III of the phase shift $\delta_1^1(s)$ (*cf.* Fig. 1), which gives the largest variation. We observe that the systematic errors attached are sizable, of about 18% and 11% for $|b|$ and ϕ_b, respectively. We also note that this value stays close to its sum-rule prediction given in Eq. (2.22). Therefore, we conclude that the pion-pion P-wave phase shift saturates the sum rule for the $J/\psi \to 3\pi$ partial wave to about 75%. This result is to be compared to similar sum rules for $\omega \to 3\pi$ in Ref. [38], where the fitted value of b was found to be quite different than its sum-rule $b_{\rm sum}$, and for $\phi \to 3\pi$ in Ref. [22], where it was observed that the difference between the fitted b and $b_{\rm sum}$ was small. The result of the fit is shown in Fig. 4 as the solid black line with the normalization of the events distribution resulting from the fits, $\mathcal{N} = 7.64(1)(33) \times 10^8$ in units of $(2.4\,\text{MeV})^{-1}$. The gray error band in the figure accounts for the systematic uncertainties associated to our calculations. It can be seen that this fit provides a satisfactory description of experimental data up to $m_{\pi\pi} \sim 1$ GeV (the elastic region). However, we obtain high values of the χ^2/dof of about 200[1] , but this problem is not critical. We shall come back to discuss this point below. Here we stress that the once-subtracted KT amplitude is able to reproduce the $\rho(770)$ function shape and note that contributions of partial waves other than the P-wave seem to be required to describe the intermediate energy region around $m_{\pi\pi} \sim 1.5$ GeV. The next allowed partial wave is the F-wave, which we will include in the following subsection. As we will see, the inclusion of an explicit F-wave improves the quality of the fit.

In Fig. 5, we show the Dalitz plot distribution resulting from our fit (the function $\phi(s,t,u)|F(s,t,u)|^2$ with $|a| = 1$ is plotted, *cf.* Eq. (2.7)), which exhibits unambiguous contributions from $\rho(770)$ resonances which appear as bands along the Dalitz plot boundaries, with almost no events in the center of the Dalitz plot. The visual comparison with the corresponding BESIII Dalitz-plot data shows a good agreement (see Fig. 2 in Ref. [3]).

3.2 Inclusion of the F-wave contribution

The isobar decomposition of the amplitude including F-waves follows from Eq. (2.8) and reads [22, 38]:

$$\begin{aligned} F(s,t,u) &= F_1(s) + F_1(t) + F_1(u) \\ &\quad + \frac{1}{16}\left[\kappa^2(s) P_3'(z_s) F_3(s) + \kappa^2(t) P_3'(z_t) F_3(t) + \kappa^2(u) P_3'(z_u) F_3(u)\right]\,, \end{aligned} \tag{3.3}$$

[1] For our analysis we have read the data points from the paper's figure and taken $\sqrt{N_{\text{events},i}}$ as the error corresponding to the i-th bin. Furthermore, we have taken into account an efficiency $\epsilon \simeq 0.3$ for the number of events and the errors.

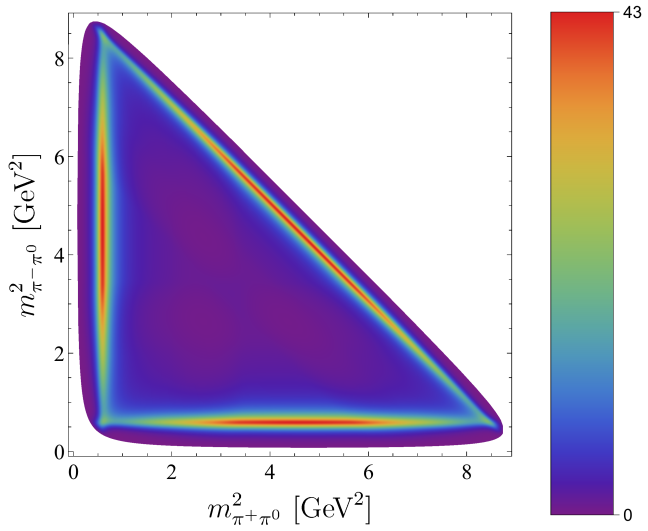

Figure 5. Dalitz plot distribution resulting from our fit in Eq. (3.2).

where $F_1(s)$ is the P-wave isobar (*cf.* Eq. (2.23a)), $\kappa(x) = \sigma_\pi(x)\lambda^{1/2}(x, m^2_{J/\psi}, m^2_\pi)$ with $\sigma_\pi(x) = \sqrt{1-4m^2_\pi/x}$, $P'_3(z)$ is the derivative of the Legendre polynomial, $F_3(x)$ is the F-wave isobar amplitude which only has a right-hand cut, and $z_t = (s-u)/\kappa(t)$, $z_u = (s-t)/\kappa(u)$. The discontinuity of the F-wave is expressed by:

$$\text{disc}\, F_3(s) = 2i\left(F_3(s) + \hat{F}_3(s)\right)\, \sin\delta_3(s)\, e^{-i\delta_3(s)}\, \theta(s-4m^2_\pi)\,, \tag{3.4}$$

where $\delta_3(s)$ and $\hat{F}_3(s)$ are the F-wave phase shift and inhomogeneity, respectively. Here, we will simplify Eq. (3.4) by neglecting $\hat{F}_3(s)$. The solution is then given by:

$$F_3(s) = p_3(s)\Omega_3(s)\,, \tag{3.5}$$

where $\Omega_3(s)$ is the F-wave Omnès function (*cf.* Eq. (2.15))

$$\Omega_3(s) = \exp\left[\frac{s}{\pi}\int_{4m^2_\pi}^{\infty}\frac{ds'}{s'}\frac{\delta_3(s')}{s'-s}\right]\,. \tag{3.6}$$

In order to obtain the required input phase $\delta_3(s)$, we model the F-wave contribution by a $\rho_3(1690)$ resonance ($J^{PC} = 3^{--}$), which can be represented by a Breit-Wigner as follows:

$$F_3(s)|_{\text{BW}} = \frac{m^2_{\rho_3}}{m^2_{\rho_3} - s - im_{\rho_3}\Gamma^{\ell=3}_{\rho_3}(s)}\,, \tag{3.7}$$

with the energy-dependent width given by

$$\Gamma^\ell_R(s) = \frac{\Gamma_R m_R}{\sqrt{s}}\left(\frac{p_\pi(s)}{p_\pi(m^2_R)}\right)^{2\ell+1}\left(F^\ell_R(s)\right)^2\,, \quad p_\pi(s) = \frac{\sqrt{s}}{2}\sigma_\pi(s)\,. \tag{3.8}$$

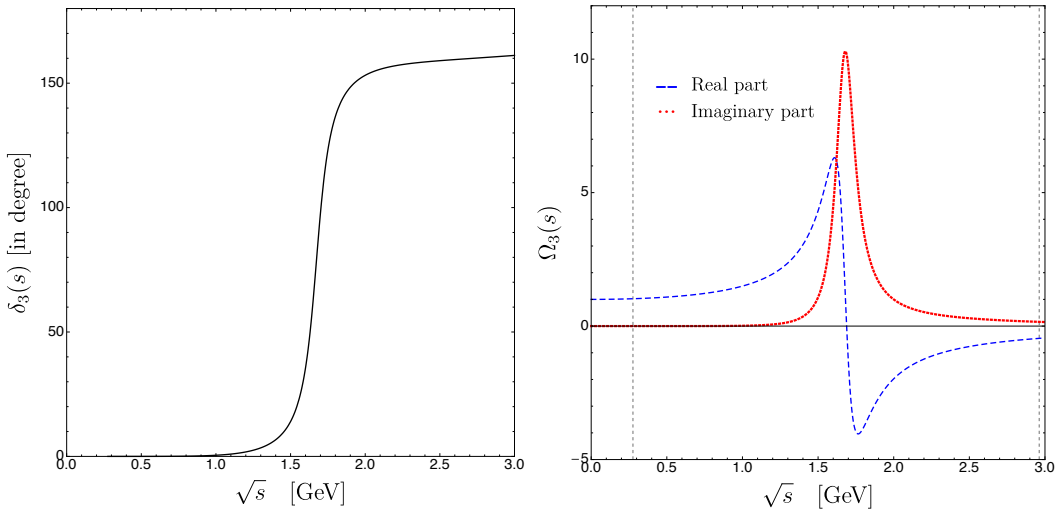

Figure 6. F-wave phase shift $\delta_3(s)$ Eq. (3.10) (left plot) and output for the Omnès function $\Omega_3(s)$ Eq. (3.6) (right plot).

The $F_R^\ell(s)$ denotes the Blatt-Weisskopf factor that limits the growth of the isobar [40]. For $\ell = 3$ it is given by:

$$F_R^{\ell=3}(s) = \sqrt{\frac{z_0(z_0-15)^2+9(2z_0-5)^2}{z(z-15)^2+9(2z-5)^2}}\,, \quad z = r_R^2 p_\pi^2(s)\,, \quad z_0 = r_R^2 p_\pi^2(m_{\rho_3}^2)\,, \tag{3.9}$$

with the hadronic scale $r_R = 2\,\text{GeV}^{-1}$.

The phase can then be computed from the relation

$$\tan\delta_3(s) = \frac{\text{Im}F_3(s)|_{\text{BW}}}{\text{Re}F_3(s)|_{\text{BW}}}\,, \tag{3.10}$$

which completes our representation of the F-wave isobar $F_3(s)$. Using $m_{\rho_3} = 1688$ MeV and $\Gamma_{\rho_3} = 161$ MeV from the PDG, in Fig. 6 we display the model for the phase $\delta_3(s)$ Eq. (3.10) and the output for the corresponding Omnès function $\Omega_3(s)$ Eq. (3.6) that we use for our analysis.

Finally, the function $p_3(s)$ in Eq. (3.5) is a polynomial that parametrizes the energy dependence not directly related to the propagation of the $\rho_3(1690)$ resonance and fixes the strength of the F-wave amplitude. In order to achieve a satisfactory description of the data, we take $p_3(s)$ linear in s with parameters relative to the P-wave amplitude, *i.e.* $p_3(s) = a(|c|e^{i\phi_c} + |d|e^{i\phi_d}\,s)$, such that the overall normalization of the amplitude a can be factored out in Eq. (3.3) and absorbed in $\mathcal{N}$ (*cf.* Eq. (3.1)) as in the previous subsection. By minimizing Eq. (3.1), we obtain the following values for the fit parameters:

$$|b| = 0.205(1)(34)\ \text{GeV}^{-2}\,, \quad \phi_b = 2.784(3)(298)\,, \tag{3.11}$$

for the P-wave subtraction constant, and

$$\begin{aligned} |c|\times 10^2 &= 4.38(1)(1.46)\ \text{GeV}^{-2}\,, & \phi_c &= 3.80(1)(5)\,, \\ |d|\times 10^2 &= 1.58(1)(46)\ \text{GeV}^{-2}\,, & \phi_d &= 0.65(1)(8)\,, \end{aligned} \tag{3.12}$$

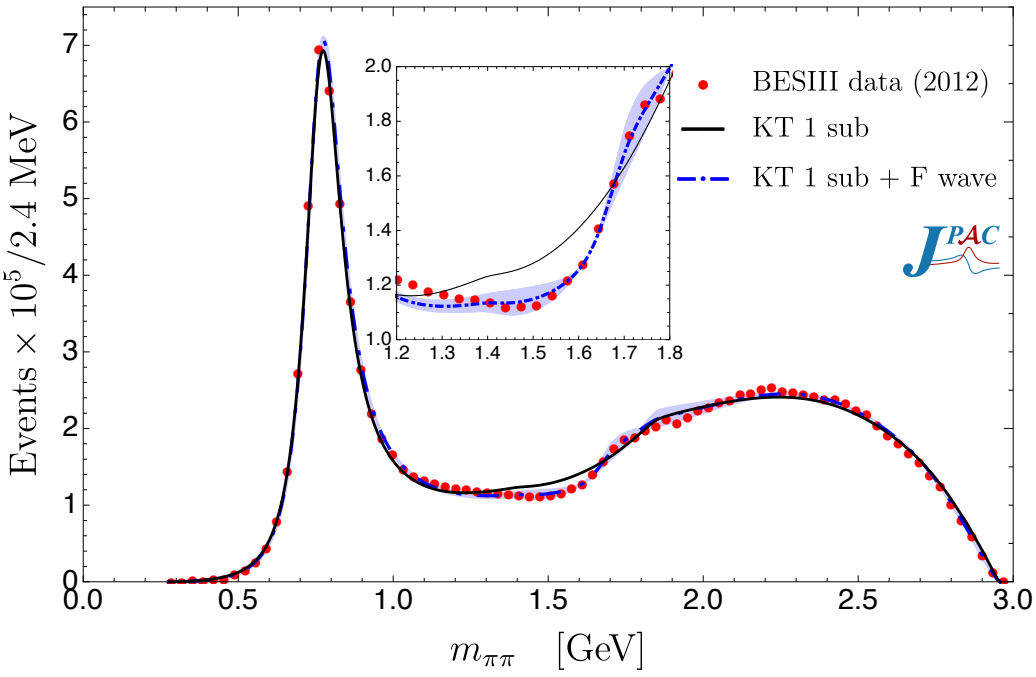

Figure 7. BESIII (red circles) [3] measurement of the $m_{\pi\pi}$ invariant mass distribution for the decay $J/\psi \to 3\pi$ as compared to our fits in Eqs. (3.2) (solid black line), (3.11) and (3.12) (dot-dashed blue line).

for the parameters of the F-wave subtracted polynomial $p_3(s)$. Again, the second error in the previous equations is the systematic uncertainty obtained from using the different P-wave phase shifts $\delta_1(s)$ as input. The result of this fit implies $|a| = 0.0581(1)(60)$ GeV^{-3} for the overall normalization of the amplitude and it is plotted in Fig. 7 as the dash-dotted blue line using the event distribution normalization from the fits, $\mathcal{N} = 8.09(1)(41) \times 10^8$ in units of $(2.4\,\text{MeV})^{-1}$. In the figure, the result of the standalone P-wave fit (*cf.* Eq.(3.2)) is also shown for comparison. As seen, the $\rho_3(1690)$-induced F-wave contribution improves the description of the data around 1.5 GeV. Numerically, we find that the individual F-wave contribution is rather small, while the interference between the P- and F-waves gives a correction of a few percent in the region $m_{\pi\pi} \sim 1.5$ GeV. The χ^2/dof remains high (about 100). However, given the systematic uncertainties associated to our fits (blue error band in Fig. 7), we conclude that our representation of the amplitude is capable of describing within errors the two more prominent features shown by the data: the line shape of the BESIII measurements in the vicinity of the $\rho(770)$ resonance as well as the movement of the function at $m_{\pi\pi} \sim 1.5$ GeV due to the F-wave effects.[2] As for the Dalitz-plot distribution, the F-wave effects provides no significant change with respect to Fig. 3.2 and we thus refrain to show them here.

[2]We shall wait for the arrival of new Dalitz distribution experimental data from BESIII to ascribe a strict statistical meaning to our χ^2 fits.

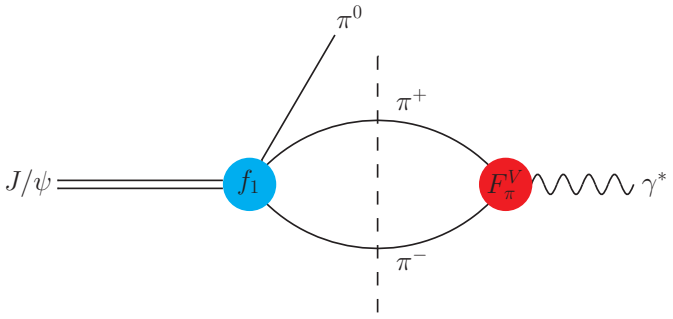

Figure 8. Diagrammatic representation of the two-pion contribution to the discontinuity of the $J/\psi\pi^0$ transition form factor [*cf.* Eq. (4.1)]. The blue and red circles represent, respectively, the full s-channel P-wave $J/\psi \to 3\pi$ amplitude $f_1(s)$ and the pion vector form factor $F_\pi^V(s)$.

4 $J/\psi \to \pi^0\gamma^*$ transition form factor

The $J/\psi\pi^0$ transition form factor (TFF), $f_{J/\psi\pi^0}(s)$, governs the $J/\psi \to \pi^0\gamma^*$ amplitude and its energy dependence is experimentally accessible from the decays $J/\psi \to \pi^0 e^+e^-$ and $J/\psi \to \pi^0\mu^+\mu^-$. At present, there is no measurement of the shape of the form factor and the only experimental information on these decays is the measurement of the branching ratio by the BESIII collaboration, $BR(J/\psi \to \pi^0 e^+e^-) = (7.56 \pm 1.32 \pm 0.50) \times 10^{-7}$ [41]. This measurement was obtained subtracting the ρ resonance contribution and assuming that the excited $c\bar{c}$ resonance contributions dominate the energy-dependence of the form factor. Refs. [28, 42] showed that subtracting this contribution is not well motivated, as the light vector meson contributions to the form factor actually dominate the decay. Using the formalism previously employed for the decays of light vector mesons $\omega/\phi \to \pi^0\gamma^*$ [24, 43], we present a dispersive description of $f_{J/\psi\pi^0}(s)$ comparable to [28], but with the difference that our analysis is driven by the $J/\psi \to 3\pi$ experimental data analysis presented in Sec. 3.

A dispersive representation of $f_{J/\psi\pi^0}(s)$ is fully determined, up to possible subtractions, by the discontinuity across the right hand cut. Here, we focus on the light-quark resonance contributions to the discontinuity, which dominate the form factor at low and intermediate energies. Additional $c\bar{c}$ contributions can arise close to the upper limit of the accessible phase space, $\sqrt{s} = m_{J/\psi} - m_{\pi^0}$, and in fact can dominate the transition form factor there [28, 42], but these contributions appear in a region of the Dalitz decays which are strongly suppressed by phase space [28, 42], rendering the task of experimentally observing them nearly impossible. Bearing this in mind, and because of the absence of experimental data for the form factor, we do not consider them in our analysis.

In order to be consistent with the elastic approximation in the $J/\psi \to \pi^+\pi^-\pi^0$ study, we include only the two-pion intermediate state contribution to the discontinuity (see Fig. 8 for a diagrammatic interpretation):

$$\text{disc} f_{J/\psi\pi^0}(s) = i\,\frac{p^3(s)}{6\pi\sqrt{s}}\,F_\pi^{V*}(s)\,f_1(s)\,\theta(s-4m_\pi^2)\,, \tag{4.1}$$

which requires as input the full s-channel P-wave $J/\psi \to 3\pi$ amplitude $f_1(s)$ given in Eq. (2.10) and the pion vector form factor complex-conjugate $F_\pi^{V*}(s)$, which we approxi-

mate by the Omnès function (complex-conjugate) given in Eq. (2.15). Given that we are using a once-subtracted dispersion relation for the $J/\psi \to 3\pi$ KT equations, an unsubtracted dispersion relation for the TFF, as used for instance in Ref. [28], would result in a divergent integral if no cutoff is used. We, therefore, use a once-subtracted dispersion relation for the TFF itself,

$$f_{J/\psi\pi^0}(s) = |f_{J/\psi\pi^0}(0)|\, e^{i\phi_{J/\psi\pi^0}(0)} + \frac{s}{12\pi^2}\int_{4m_\pi^2}^{\infty} \frac{ds'}{(s')^{3/2}} \frac{p^3(s')\, F_\pi^{V\,*}(s')\, f_1(s')}{(s'-s)}\,, \tag{4.2}$$

where we indicate explicitly the existence of a non-vanishing phase of $f_{J/\psi\pi^0}(s)$ at $s = 0$. This is implied by the cross-channel effects, *i.e.* the functions $F_\pi^{V\,*}(s)$ and $f_1(s)$ do not have the same phase, and the discontinuity of $f_{J/\psi\pi^0}(s)$ is in general complex [24, 43]. The modulus of the subtraction constant $|f_{J/\psi\pi^0}(0)|$ can be fixed from the $J/\psi \to \pi^0\gamma$ partial decay width

$$\Gamma(J/\psi \to \pi^0\gamma) = \frac{e^2(m_{J/\psi}^2 - m_{\pi^0}^2)^3}{96\pi m_{J/\psi}^3}\, |f_{J/\psi\pi^0}(0)|^2\,. \tag{4.3}$$

Using the PDG value for $J/\psi \to \pi^0\gamma$ [39] in combination with the above equation, one obtains:

$$|f_{J/\psi\pi^0}(0)| = 6.0(3) \times 10^{-4} \quad \text{GeV}^{-1}\,. \tag{4.4}$$

The phase $\phi_{J/\psi\pi^0}(0)$ is a free parameter that can only be accessed from the transition form factor experimental data (see *e.g.* [24]). Due to the absence of data for $J/\psi \to \pi^0\gamma^*$, we set $\phi_{J/\psi\pi^0}(0) = 0$ in our study.

In Fig. 9, we show our prediction for the absolute value of the transition form factor resulting from Eq. (4.2) up to $\sqrt{s} = 2$ GeV (solid black line). In this figure, we also show the result of using the unsubtracted KT solution for $J/\psi \to 3\pi$ (dashed blue line). It is worth noting that both curves are similar and only a slight difference is observed at the ρ peak. Additionally, the calculations when an unsubtracted dispersion relation for the form factor is used are also shown in the figure, both with an unsubtracted (dotted red line) and once-subtracted (dot-dashed green line) $J/\psi \to 3\pi$ amplitude. In the latter case, we have cut the dispersive integral at 4 GeV^2 to avoid the dispersion relation to diverge. Again, both curves are similar. In this case, the value at the real photon energy can be calculated from the sum rule [28, 43]:

$$f_{J/\psi\pi^0}(0) = \frac{1}{12\pi^2}\int_{4m_\pi^2}^{\infty} ds' \frac{p^3(s') F_\pi^{V\,*}(s') f_1(s')}{(s')^{3/2}}\,. \tag{4.5}$$

This value is found to be $|f_{J/\psi\pi^0}(0)| \approx 5.0 \times 10^{-4}$ GeV^{-1}, for both versions of the unsubtracted dispersion relation, and is in qualitative agreement with the value extracted from the measured $J/\psi \to \pi^0\gamma$ in Eq. (4.4), indicating that the normalization is saturated by the two-pion intermediate state contribution by roughly 85%. The difference between the various lines provides an estimate of the theoretical uncertainty associated to our description. We expect our study to strengthen the case for new experimental measurements of the shape of this form factor, which would allow improving the understanding of radiative J/ψ decays.

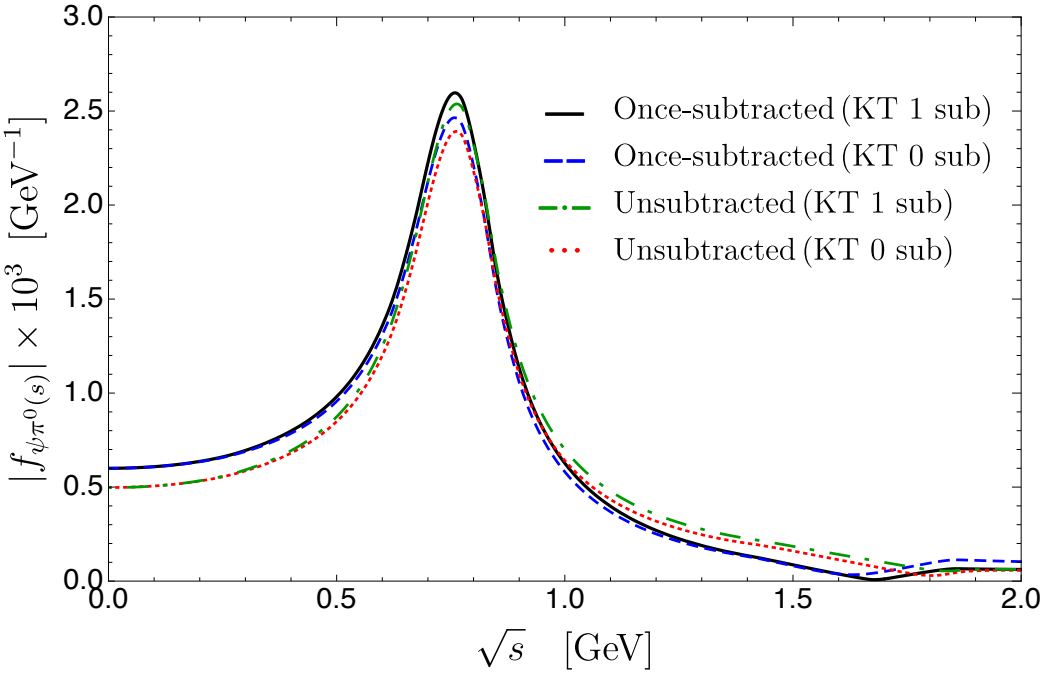

Figure 9. Prediction for the absolute value of the transition form factor $J/\psi \to \pi^0\gamma^*$ using Eq. (4.2) (solid black line) and variants of it. See main text for details.

5 Summary

We have analyzed the decay $J/\psi \to \pi^+\pi^-\pi^0$ within the framework of the Khuri-Treiman equations, which satisfy the constraints imposed by unitarity, analyticity and crossing symmetry. We have included the P-wave effects of the $\pi\pi$ subsystem up to around 2 GeV, which are controlled by the $\pi\pi$ P-wave scattering-phase shift. We have seen that one subtraction in the P-wave amplitude is necessary to achieve a good description ot the experimental data in the $\rho(770)$-region. The corresponding subtraction constant, which is complex, was fixed from fits to the di-pion invariant mass distribution from BESIII. We have also seen that the P-wave alone is not capable of reproducing the data in the mass region around $m_{\pi\pi} \sim 1.5$ GeV, and that the inclusion of an F-wave contribution arising from the $\rho_3(1690)$ brings theory closer to data in this region. In addition, we have provided predictions for the transition form factor $J/\psi \to \pi^0\gamma^*$ up to 2 GeV. Our study lays the groundwork for an event-by-event likelihood fit of high-precision data from J/ψ decays, which will soon be available from BESIII.

Acknowledgments

The authors would like to thank Joshua Jackson and Ryan Mitchell (Indiana University) for fruitful discussions. MA is supported by Generalitat Valenciana under Grant No. CIDEGENT/2020/002. The work of SGS is supported by the Laboratory Directed Research and Development program of Los Alamos National Laboratory under project

number 20210944PRD2, and by the U.S. Department of Energy through the Los Alamos National Laboratory. Los Alamos National Laboratory is operated by Triad National Security, LLC, for the National Nuclear Security Administration of U.S. Department of Energy (Contract No. 89233218CNA000001). This work was supported by the U.S. Department of Energy contract DE-AC05-06OR23177, under which Jefferson Science Associates, LLC operates Jefferson Lab, U.S. Department of Energy Grants No. DE-FG02-87ER40365 and No. DE-FG02-92ER40735, CONACYT (Mexico) Grant No. A1-S-21389, and Spanish national Grants PID2020-118758GB-I00 and PID2019–106080 GB-C21. CFR is supported by Spanish Ministerio de Educación y Formación Profesional under Grant No. BG20/00133. VM is a Serra Húnter fellow. This work is also supported in part within the framework of the ExoHad Topical Collaboration.

References

[1] J. Z. Bai *et al.* (BES), Phys. Rev. D **70**, 012005 (2004), arXiv:hep-ex/0402013.

[2] B. Aubert *et al.* (BaBar), Phys. Rev. D **70**, 072004 (2004), arXiv:hep-ex/0408078.

[3] M. Ablikim *et al.* (BESIII), Phys. Lett. B **710**, 594 (2012), arXiv:1202.2048 [hep-ex].

[4] Y.-Q. Chen and E. Braaten, Phys.Rev.Lett. **80**, 5060 (1998), arXiv:hep-ph/9801226.

[5] X.-H. Mo, C.-Z. Yuan, and P. Wang, Chin.Phys. **C31**, 686 (2007), arXiv:hep-ph/0611214.

[6] Q. Wang, G. Li, and Q. Zhao, Phys.Rev. **D85**, 074015 (2012), arXiv:1201.1681 [hep-ph].

[7] N. Kivel, (2023), arXiv:2301.03884 [hep-ph].

[8] L.-W. Yan, Y.-H. Chen, C.-G. Duan, and Z.-H. Guo, (2023), arXiv:2301.03869 [hep-ph].

[9] M. Ablikim *et al.* (BESIII), Chin. Phys. C **46**, 074001 (2022), arXiv:2111.07571 [hep-ex].

[10] M. Ablikim *et al.* (BESIII), Chin. Phys. C **44**, 040001 (2020), arXiv:1912.05983 [hep-ex].

[11] A. P. Szczepaniak and M. R. Pennington, Phys.Lett. **B737**, 283 (2014), arXiv:1403.5782 [hep-ph].

[12] P. Guo, R. Mitchell, and A. P. Szczepaniak, Phys.Rev. **D82**, 094002 (2010), arXiv:1006.4371 [hep-ph].

[13] P. Guo, R. Mitchell, M. Shepherd, and A. P. Szczepaniak, Phys.Rev. **D85**, 056003 (2012), arXiv:1112.3284 [hep-ph].

[14] N. N. Khuri and S. B. Treiman, Phys. Rev. **119**, 1115 (1960).

[15] A. V. Anisovich and H. Leutwyler, Phys. Lett. **B375**, 335 (1996), arXiv:hep-ph/9601237 [hep-ph].

[16] P. Guo, I. Danilkin, and A. P. Szczepaniak, Eur. Phys. J. A **51**, 135 (2015), arXiv:1409.8652 [hep-ph].

[17] P. Guo, I. V. Danilkin, D. Schott, C. Fernández-Ramírez, V. Mathieu, and A. P. Szczepaniak, Phys. Rev. **D92**, 054016 (2015), arXiv:1505.01715 [hep-ph].

[18] G. Colangelo, S. Lanz, H. Leutwyler, and E. Passemar, Phys. Rev. Lett. **118**, 022001 (2017), arXiv:1610.03494 [hep-ph].

[19] G. Colangelo, S. Lanz, H. Leutwyler, and E. Passemar, Eur. Phys. J. **C78**, 947 (2018), arXiv:1807.11937 [hep-ph].

[20] M. Albaladejo and B. Moussallam, Eur. Phys. J. **C77**, 508 (2017), arXiv:1702.04931 [hep-ph].

[21] J. Gasser and A. Rusetsky, Eur. Phys. J. **C78**, 906 (2018), arXiv:1809.06399 [hep-ph].

[22] F. Niecknig, B. Kubis, and S. P. Schneider, Eur. Phys. J. **C72**, 2014 (2012), arXiv:1203.2501 [hep-ph].

[23] I. V. Danilkin, C. Fernández-Ramírez, P. Guo, V. Mathieu, D. Schott, M. Shi, and A. P. Szczepaniak, Phys. Rev. **D91**, 094029 (2015), arXiv:1409.7708 [hep-ph].

[24] M. Albaladejo, I. Danilkin, S. Gonzàlez-Solís, D. Winney, C. Fernández-Ramírez, A. Hiller Blin, V. Mathieu, M. Mikhasenko, A. Pilloni, and A. Szczepaniak, Eur.Phys.J. **C80**, 1107 (2020), arXiv:2006.01058 [hep-ph].

[25] G. Källén, *Elementary particle physics* (Addison-Wesley, Reading, MA, 1964).

[26] T. W. B. Kibble, Phys. Rev. **117**, 1159 (1960).

[27] M. Albaladejo *et al.* (JPAC), Prog. Part. Nucl. Phys. **127**, 103981 (2022), arXiv:2112.13436 [hep-ph].

[28] B. Kubis and F. Niecknig, Phys. Rev. D **91**, 036004 (2015), arXiv:1412.5385 [hep-ph].

[29] D. Stamen, T. Isken, B. Kubis, M. Mikhasenko, and M. Niehus, (2022), arXiv:2212.11767 [hep-ph].

[30] M. Albaladejo, D. Winney, I. Danilkin, C. Fernández-Ramírez, V. Mathieu, M. Mikhasenko, A. Pilloni, J. Silva-Castro, and A. Szczepaniak (JPAC), Phys. Rev. D **101**, 054018 (2020), arXiv:1910.03107 [hep-ph].

[31] J. B. Bronzan and C. Kacser, Phys.Rev. **132**, 2703 (1963).

[32] R. Omnes, Nuovo Cim. **8**, 316 (1958).

[33] M. Froissart, Phys. Rev. **123**, 1053 (1961).

[34] A. Martin, Phys. Rev. **129**, 1432 (1963).

[35] J. R. Pelaez, A. Rodas, and J. Ruiz De Elvira, Eur. Phys. J. C **79**, 1008 (2019), arXiv:1907.13162 [hep-ph].

[36] S. Gonzàlez-Solís and P. Roig, Eur. Phys. J. C **79**, 436 (2019), arXiv:1902.02273 [hep-ph].

[37] R. Garcia-Martin, R. Kaminski, J. R. Pelaez, J. Ruiz de Elvira, and F. J. Yndurain, Phys. Rev. D **83**, 074004 (2011), arXiv:1102.2183 [hep-ph].

[38] M. Albaladejo, I. Danilkin, S. Gonzalez-Solis, D. Winney, C. Fernandez-Ramirez, A. N. H. Blin, V. Mathieu, M. Mikhasenko, A. Pilloni, and A. Szczepaniak (JPAC), Eur. Phys. J. C **80**, 1107 (2020), arXiv:2006.01058 [hep-ph].

[39] R. L. Workman and Others (Particle Data Group), PTEP **2022**, 083C01 (2022).

[40] J. M. Blatt and V. F. Weisskopf, *Theoretical nuclear physics* (Springer, New York, 1952).

[41] M. Ablikim *et al.* (BESIII), Phys. Rev. D **89**, 092008 (2014), arXiv:1403.7042 [hep-ex].

[42] Y.-H. Chen, Z.-H. Guo, and B.-S. Zou, Phys. Rev. D **91**, 014010 (2015), arXiv:1411.1159 [hep-ph].

[43] S. P. Schneider, B. Kubis, and F. Niecknig, Phys. Rev. D **86**, 054013 (2012), arXiv:1206.3098 [hep-ph].